

Ab Initio Modeling of Amide-Stabilized, Oligo(ethylene glycol)-Terminated Self-Assemblies: In-SAM Molecular Geometry, Orientation, and Hydrogen Bonding

Lyuba Malysheva,[†] Alexander Onipko,^{†,‡} and Bo Liedberg^{*,‡}

Bogolyubov Institute for Theoretical Physics, 03680 Kyiv, Ukraine, and Division of Molecular Physics, Department of Physics, Chemistry and Biology, Linköping University, S-581 83 Linköping, Sweden

Received: December 10, 2007; In Final Form: January 15, 2008

Under the constraint that sulfur atoms form a hexagonal ($\sqrt{3} \times \sqrt{3}$)R30° overlay on the (111) gold surface, the optimized geometry of periodic arrays of HS(CH₂)₃CONH–(CH₂CH₂O)₃H molecules has been found ab initio, by exploiting the BP86 exchange–correlation functional with 6-31G and “general” basis sets. The obtained data suggests that several prominent features of in-SAM molecular geometry and orientation stand out from conclusions based on single-molecule modeling. In particular, changing of amide-related dihedrals is shown to dominate in adjustment of molecular constituents to the assembly environment and to result in a substantial shortening of the hydrogen bond distance between nearest-neighbor amides. First demonstrated here, the full account to the intermolecular interaction within periodic arrays of amide-bridged, oligo(ethylene glycol)-terminated alkanethiolates forms a new platform for arguable modeling of SAM apparent properties.

1. Introduction

This letter reports on molecular geometry and orientation within self-assembled monolayers (SAMs) of amide-stabilized, oligo(ethylene glycol) (OEG)-terminated alkanethiolates, as it is predicted by the first-principle modeling of hexagonal periodic arrays of HS–(CH₂)₃–CONH–(CH₂CH₂O)₃–H molecules. The obtained results are pertinent to several debated issues such as the internal microscopic structure of SAMs,^{1–3} mechanisms of SAM stability,^{4–6} and SAM surface properties.^{7–10} The accurate account to the intermolecular interaction in SAM-relevant periodic arrays is also a vital step toward developing reliable microscopic models of water interaction with OEGs. In this respect, the presented model can be regarded as a prototype of a “dry” OEG-terminated SAM suitable for further ab initio studies of water adsorption and wetting mechanisms.

The choice of the model system has been guided by the following considerations. First, this family of self-assemblies demonstrates high ordering and stability in a temperature range where two dominating OEG conformations have been observed: helical at room temperature, and all-trans at temperatures near 65 °C.^{11,12} In between these temperatures, the OEG adopts a disordered, amorphous-like conformation. Despite a comparatively short history, this family of SAMs has an impressive record of applications as templates for model membranes,^{13,14} protein-resistant surfaces,^{8,15,16} and a variety of fancy materials for submicron sensing and electronics.^{17,18} The aim of this modeling is to advance fundamentals of this development.

Second, this study has been preceded by a combined theoretical and experimental effort pointed at the relationship

between, on one hand, the ab initio calculated geometry, vibration frequencies, and transition dipole moments of SAM molecular constituents, HS–(CH₂)_m–CONH–(CH₂CH₂O)_n–H, $m = 15, n = 4, 6$; $m = 11, n = 6$, and, on the other hand, their appearance in experimental spectra.^{11,12,19} We have succeeded in obtaining excellent agreement between experimental and calculated infrared reflection absorption (IR RA) spectra for a given molecular orientation. In particular, the OEG orientation has been shown to be far from the up-right standing with regard to the substrate, as is often postulated in the “idealized model” of OEG-terminated SAMs.^{7,20} However, all our previous conclusions regarding the in-SAM molecular orientation¹⁹ relied on the experimental data and calculations for isolated molecules. This first-principle modeling is intended to shed some light on the role of intermolecular interactions in SAM formation.

2. Calculation Essentials

We are particularly interested in changes of intra- and intermolecular structure associated with formation of favorable hydrogen bonding geometries and molecular orientation(s), which is adopted within SAMs of amide-bridged, OEG-terminated alkanethiolates. To the best of our knowledge, there are no evidence that, in experimentally investigated SAMs, these characteristics are significantly dependent on numbers of methylene and/or ethylene-glycol units. In our model SAMs, both are set equal to three; larger numbers lead to an enormous increase of computational time.

Initial Geometry and Orientation. The geometry optimization was started from a hexagonal periodic array of HS(CH₂)₃–CONH–(CH₂CH₂O)₃H molecules, where sulfur atoms of the nearest neighbors are separated by 5 Å, and the OEG portion has either helical (h) or all-trans (t) configuration. An example of such a structure is illustrated in Figure 1 by a nine-member

* To whom correspondence should be addressed. E-mail: bol@ifm.liu.se.

[†] Bogolyubov Institute for Theoretical Physics.

[‡] Linköping University.

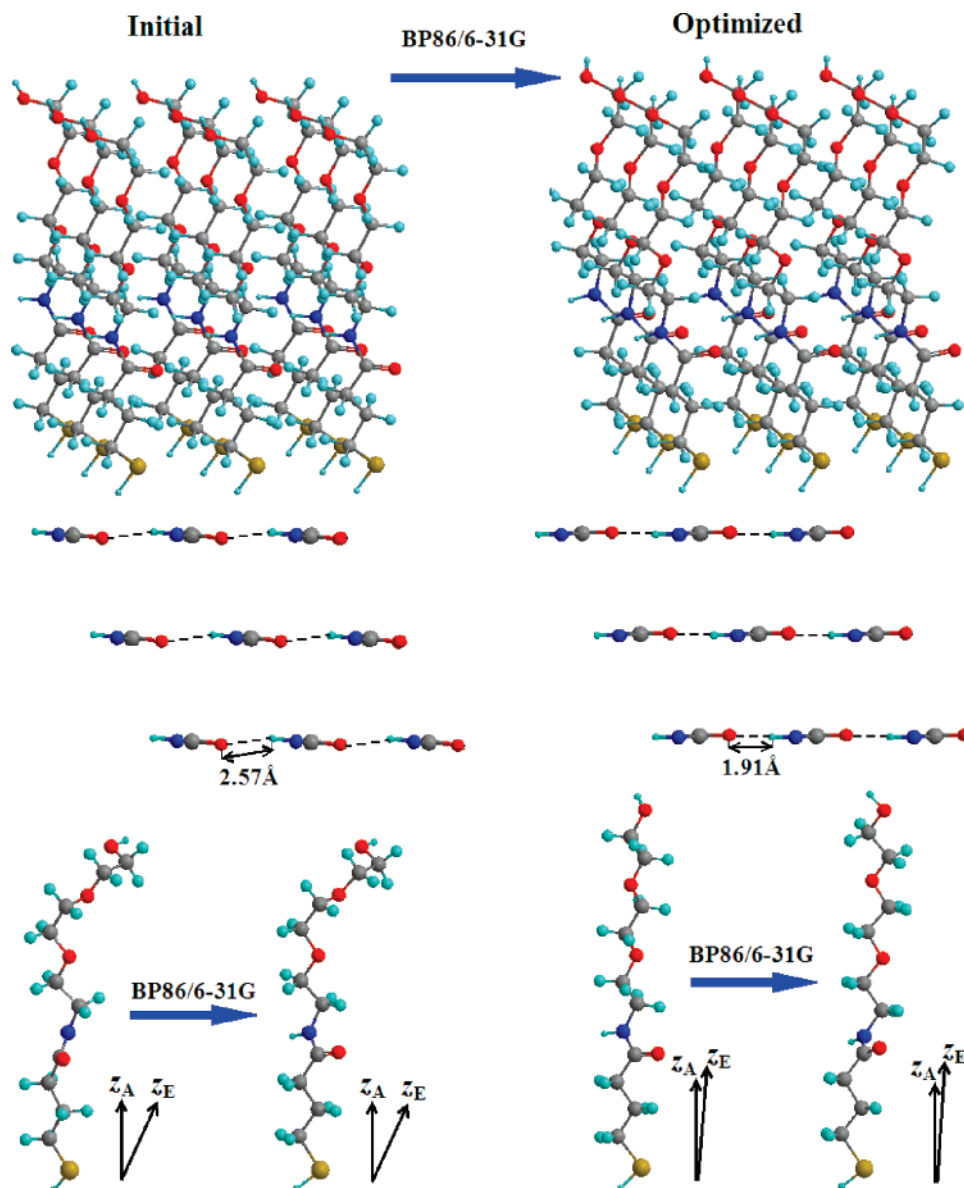


Figure 1. Upper panel: 3×3 periodic structure of $\text{HS}(\text{CH}_2)_3\text{CONH}-(\text{CH}_2\text{CH}_2\text{O})_3\text{H}$ molecules before and after optimization; OEG is in helical conformation. Lower panel: same changes (except real tilt of z_A axis) are shown for a molecule within periodic arrays in helical (left) and all-trans (right) conformations. Optimization of the lateral hydrogen bonding within the structure (chains of amide groups couple to each other via $\text{H}\cdots\text{O}$ bonds) is illustrated in the middle panel.

periodic array of h molecules. In the process of optimization, the S–S distance was kept fixed, whereas all bonds, bond angles and dihedrals were free to change. Thus, we assume that sulfur atoms of the molecules h and t form hexagonal ($\sqrt{3} \times \sqrt{3}$)R30° lattices, and our purpose is to find equilibrium geometries of respective periodic arrays of h and t molecules. The admitted periodicity is supported by a multitude of experimental facts and seems to be a reasonable starting point of the first ab initio modeling of the self-assemblies in focus.

Designed as an idealized prototype of the amide-stabilized SAMs mentioned in the Introduction, periodic arrays of h and t molecules were optimized with such initial geometry and orientation that provides the best fit with IR RA spectroscopy data on SAMs of $\text{HS}(\text{CH}_2)_{15}\text{CONH}-(\text{CH}_2\text{CH}_2\text{O})_6\text{H}$ molecules.^{19,21} In quoted works, the molecule optimized geometry, vibration frequencies, and transition dipole moments were obtained at the DFT level with gradient corrections. From the quantitative comparison of simulated SAM RA spectra with experiment (briefly summarized below), an optimal molecular orientation has been deduced, reproducing relative intensities

of characteristic peaks and giving the minimal $\text{H}\cdots\text{O}$ distance between nearest-neighbor amide groups in the range of 2.3–2.6 Å.

With respect to the xy plane, coinciding with the hexagonal lattice of S atoms, the molecular orientation is determined by Euler angles θ_A (tilt of z_A axis), ψ_A (rotation of alkyl CCC plane about z_A axis), and azimuthal angle φ_A , see Figure 2. The initial values of these angles and the corresponding Euler angles for the amide and OEG components are shown in Table 1. These parameters are consistent with the observed relative intensity of the alkyl symmetric and asymmetric peaks in the CH-stretching region (depends on θ_A and ψ_A); the bands of C=O and N–H stretching vibrations (amide I and amide A bands) do not show up in the IR RA spectrum (angles $\gamma_{\text{C=O}}$ and $\gamma_{\text{N-H}}$ are close to 90°), whereas the band of combined C–N–H in-plane bending and C–N stretching vibrations (amide II band) gives an intense peak in the RA spectrum (angle θ_N is not close to 90°); azimuthal angle φ_A provides the minimal (and not contradicting to other limitations) $\text{H}\cdots\text{O}$ distance between oxygen and hydrogen of the nearest-neighbor amide groups.

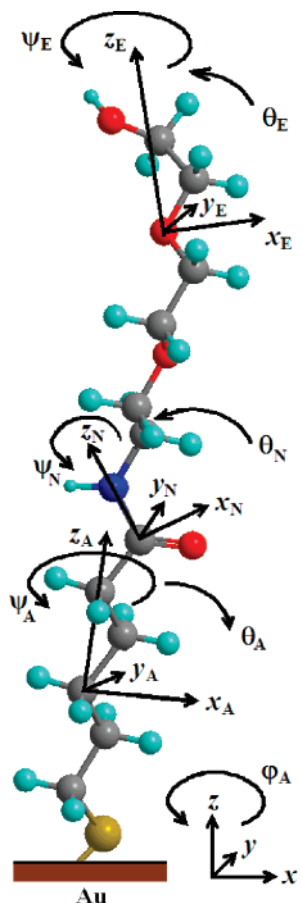


Figure 2. Definition of Euler angles, tilt θ_a about the z -axis, $x_a y_a$ plane rotation ψ_a about the z_a axis, and azimuthal angle φ_a about the z -axis ($a = A, E, N$) for $(\text{CH}_2)_3$ alkyl (A), $(\text{CH}_2\text{CH}_2\text{O})_3$ OEG (E), and CONH amide (N) segments of the $\text{HS}(\text{CH}_2)_3\text{CONH}-(\text{CH}_2\text{CH}_2\text{O})_3\text{H}$ molecule.

TABLE 1: Initial^a and Optimized^b Molecular Orientation for a Hexagonal Periodic Array of $\text{HS}-(\text{CH}_2)_3-\text{CONH}-(\text{CH}_2\text{CH}_2\text{O})_3-\text{H}$ Molecules with OEG in Helical (h) and All-Trans (t) Conformations

Euler angles (in degrees)	$\theta_A, \psi_A, \varphi_A$	$\theta_E, \psi_E, \varphi_E$	$\theta_N, \psi_N, \varphi_N$	$\gamma_{\text{C=O}}^c$	$\gamma_{\text{N-H}}^d$
initial	h 26, -62, -77	22, 25, -151	-27, -4, -3	95	89
	t 26, -65, -82	32, -38, -73	-36, -3, 4	94	90
optimized	h 25, -38, -85	13, 25, -175	-42, -4, 5	81	103
6-31G basis	t 12, -44, -75	21, -41, -55	-47, 28, -19	80	104
optimized	h 29, -43, -76	16, 24, -169	-41, -3, 4	82	102
general basis	t 17, -35, -73	21, -42, -56	-47, 26, -18	79	104

^a Values of alkyl (A), OEG (E), and amide (N) Euler angles are the same as those in ref 19; these angles are defined in Figure 2. ^b DFT BP86 method with 6-31G and general basis sets (see text). ^c Angle between the C=O bond and the z -axis. ^d Angle between the N-H bond and the z -axis.

Methodology. From our own and others experience,^{20,21} we know that the BP86 exchange-correlation functional with 6-31G basis set is sufficient for a reliable reproduction of the geometry of organic molecules in focus. Further extension of the basis, for example, taking into account d orbitals, as it does the 6-31G* basis, usually gives insignificant corrections. Nevertheless, for better control of the simulated geometry, after optimization with the 6-31G basis, the calculation procedure was repeated again, employing the so-called general basis. In the latter basis, the OEG part (except hydrogen) was described by 6-31G*, CONH group was calculated at 6-31G level, and 3-21G basis was used for the alkyl chain and all hydrogen atoms. The array geometry obtained with BP86 6-31G was used as the initial for calcula-

tions with the general basis that includes d orbitals for the OEG part. Furthermore, the reliability of optimization procedure was ensured by using two initial molecular geometries: the non-equilibrium and equilibrium free-molecule geometry. Both led to the same results. The standard optimization routine of optimization with periodic boundary conditions, as provided by the Gaussian 03 package, was used in all calculations.

3. Results and Discussion

Tables 1 and 2 display the initial and optimized geometries and orientations of $\text{HS}-(\text{CH}_2)_3-\text{CONH}-(\text{CH}_2\text{CH}_2\text{O})_3-\text{H}$ molecules within the hexagonal periodic array. As already mentioned, the optimization of SAM geometry has been performed for helical and all-trans conformations of the OEG part. A general conclusion is that adjustment of molecules to the SAM environment requires specific changes in the molecular geometry and orientation.

Free Molecule versus In-SAM Molecular Orientation. As seen from Table 1, optimization (that is to say, “switching on” the intermolecular interaction) has a profound effect on the molecular orientation, which depends on the conformational state. Also, the effect is different for the alkyl, amide, and OEG parts of molecules. For example, the tilt of an alkyl CCC plane decreases by $\sim 10-15^\circ$ in t-arrays, whereas the change in ψ_A is about 20° for both conformations. The noticeably smaller alkyl tilt for the array in all-trans conformation concurs with the decrease of the intensity of the band of C-H asymmetric stretching vibrations that was recorded under helical-all-trans transition in SAMs of $\text{HS}-(\text{CH}_2)_{15}-\text{CONH}-(\text{CH}_2\text{CH}_2\text{O})_6-\text{H}$.¹² Other trends of this modeling worth mentioning are the decrease of OEG tilt and the substantial changes in the orientation of amide group. The former indicates the net straightening effect of the environment on this type of molecule; the latter results in a substantial decrease of H \cdots O length in the h- and t-arrays after optimization of the array geometry (see Table 2).

The calculated molecular orientation within the model SAMs of h and t molecules implies a somewhat different appearance of the RA spectrum in comparison with that which would have the h- or t-array in its initial geometry. However, a detailed inspection of changes in angles θ and ψ for the alkyl, amide, and OEG structural parts shows that, in the main features, the spectrum description given by the previous single-molecule modeling^{19,21} is correct.

Free Molecule versus In-SAM Molecular Geometry. Further, we can trace the microscopic origins of changes in the initial molecular orientation by comparing the geometry before and after optimization. In Table 2, represented in columns “free” and “in-SAM” are optimized geometries of free h and t molecules and the geometries, which these molecules acquire under the influence of the intermolecular interaction within a hexagonal lattice with 5 Å spacing. These calculations show that the most substantial difference between the in-SAM and free molecular geometries are associated with the amide bridge. The usage of both basis sets support the conclusion that, for a free and in-SAM molecule, changing of initial CONH-related dihedrals is driven in the opposite directions. In other words, if, in the free molecule, any of these angles decreases/increases, the combined effect from intra- and intermolecular interactions results in the increase/decrease of the angle, and vice versa. Probably, the most remarkable is that these opposite changes are well comparable in magnitude, showing that the prescribed initial geometry is halfway from the free molecule equilibrium geometry to the geometry within the assembly. To recall, the

TABLE 2: Characteristic Dihedrals^a of HS-(CH₂)₃-CONH-(CH₂CH₂O)₃-H Molecules in Helical (h) and All-Trans (t) Conformations

dihedrals (in degrees)	initial h (t)	in-SAM h (t)		free h (t)	
		BP86 6-31G	general	BP86 6-31G	general
$\tau^{\perp}(\text{OCCO})$	72 (180)	72 (170)	70 (170)	78 (180)	73 (180)
$\tau(\text{OCCO})$	71 (179)	77 (177)	71 (178)	77 (179)	72 (179)
$\tau(\text{CCCC})$	172 (174)	174 (177)	177 (173)	171 (171)	171 (171)
$\tau(\text{CNCC})$	-105 (-103)	-114 (-106)	-114 (-106)	-96 (-97)	-99 (-101)
$\tau(\text{CCCN})$	133 (135)	126 (115)	117 (103)	142 (141)	143 (141)
$\tau(\text{CCCO})$	-47 (-45)	-55 (-64)	-63 (-75)	-38 (-40)	-38 (-40)
$d(\text{H}\cdots\text{O})^b$ (Å)	2.57 (2.46)	1.91 (1.87)	1.93 (1.85)		
$\angle(\text{N}-\text{H}\cdots\text{O})^c$	153 (155)	177 (179)	176 (180)		

^a Labeling of dihedrals: at the OEG terminus, $\tau^{\perp}(\text{OCCO})$; for OCCO and CCCC groups, which are the nearest-neighbors of amide from the side of OEG and alkyl, respectively; amide-related dihedrals, $\tau(\text{CNCC})$, $\tau(\text{CCCN})$, and $\tau(\text{CCCO})$, which determine the relative orientation of the alkyl and OEG parts. ^b Length of H \cdots O bond. ^c Angle between N-H and H \cdots O bonds.

nonequilibrium initial geometries of h and t molecules are exact copies of the corresponding part of the HS-(CH₂)₁₅-CONH-(CH₂CH₂O)₆-H molecule in the respective conformational states. Our calculations show that this choice fits the assembly environment better than it does the optimized geometry of h and t molecules.

As mentioned above, this modeling suggests different alkyl tilts for SAMs in helical (larger) and all-trans (smaller) conformations. It also intimates that, within the SAM, the all-trans OEG conformation undergoes certain deformation. Dihedrals, which, in the free molecule state, are all close to 180°, deviate from this value up to 15°, exposing the overall tendency toward bending of the OEG-chain (not represented in the illustrative material). It might be a peculiar kind of molecular disorder provoked by the intermolecular interaction. At least, it never appears in the free state of the all-trans OEG conformation. Regarding this and other implications of the reported results, other models of OEG-containing SAMs should be studied at the ab initio level.

Hydrogen Bonding. Comparing the initial and optimized length of the H \cdots O distance (see $d(\text{H}\cdots\text{O})$) and related amide parameters in Table 2), it becomes obvious that it is the creation of hydrogen-bonding that plays the major role in adjusting of the amide (and the whole molecule) to the specific in-SAM geometry. As a result, the characteristic hydrogen-bonding length establishes; $d(\text{H}\cdots\text{O})$ is about 1.9 Å in both h- and t-arrays. For periodic arrays with the OEG component in helix and all-trans conformations, the obtained decrease of total electronic energies per molecule is 18.5 and 17 kcal/mol, respectively. A larger part of this energy gain is due to an increased polarity of amide groups and hydrogen bond formation. The latter can be roughly estimated by a value of ~ 10 kcal/mol.

The observed decrease in the alkyl tilt within the model SAM is, most likely, due to amide bridge directing force. At least, there is no other reasonable explanation why the periodic array without the amide and OEG parts, which is optimized by the same method, gives $\theta_A \sim 20^\circ$. Thus, it is the presence of the amide, connecting the molecule alkyl and OEG parts and forming chains of hydrogen bonds parallel to the *xy* (SSS) plane, that makes the molecular geometry within the SAM distinct in many aspects from the geometry when these molecules are free. We expect therefore, that, in self-assemblies, where alkyl and OEG chains are connected via ester or ether linkage, the in-SAM molecular geometry has another form, likely, much more similar to the free state geometry.

Summarizing, as a model of self-assemblies of OEG-terminated, amide-bridged alkanethiolates on Au (111), the optimized structure of hexagonal periodic arrays of HS(CH₂)₃-

CONH-(CH₂CH₂O)₃H molecules in helical and all-trans conformations is obtained by the DFT BP86 method. In the resulting structure, the strong hydrogen bonding is formed, connecting nearest neighbor amides via H \cdots O bonds (~ 1.9 Å), which are somewhat longer for the helical conformation. This quantifies earlier experimental findings regarding amide-stabilized OEG-terminated self-assemblies.^{11,12} Details of the molecular geometry and orientation within ab initio optimized periodic arrays are compared with the data of single-molecule modeling. This analysis has disclosed several distinctions between the free molecule and in-SAM molecule geometries, showing how the molecular orientation changes when affected by the SAM environment. However, we expect that, under the obtained changes in the Euler angles, the shape of SAM RA spectra, which was previously calculated at the single-molecule level,¹⁹ will be essentially the same, because the effect of van der Waals intermolecular interaction on actual intramolecular characteristics is, as a rule, small.

The most significant is the difference in the amide-related dihedrals that are adjusting to the assembly environment in a way that is best suitable for forming interamide hydrogen bonding. As a result, the shortest possible H \cdots O distance in the periodic arrangement of non-interacting molecules is reduced by ~ 0.6 Å. This can be considered as a net effect of the intermolecular interaction. Changes in the amide bridge directing dihedrals result in a reorientation of the alkyl and OEG parts of SAM constituents. The present modeling of the interior of amide-stabilized, OEG-terminated SAMs has improved our understanding of this family of self-assemblies and makes future ab initio studies of their interaction with water and other adsorbate molecules justified and worth pursuing.

Acknowledgment. This work was supported by the Swedish Foundation for Strategic Research (SSF), the Swedish Research Council (VR), the Visby program (SI), and the Royal Academy of Science (KVA).

References and Notes

- (1) Prime, K. L.; Whitesides, G. M. *Science* **1991**, 252, 1164.
- (2) Ulman, A. *Chem. Rev.* **1996**, 96, 1533.
- (3) Love, J. C.; Estroff, L. A.; Kriebel, J. K.; Nuzzo, R. G.; Whitesides, G. M. *Chem. Rev.* **2005**, 105, 1103.
- (4) Laibinis, P. E.; Whitesides, G. M.; Allara, D. L.; Tao, Y.-T.; Parikh, A. N.; Nuzzo, R. G. *J. Am. Chem. Soc.* **1991**, 113, 7152.
- (5) Schreiber, F. *Prog. Surf. Sci.* **2000**, 65, 151.
- (6) Vanderah, D. J.; Arsenault, J.; La, H.; Gates, R. S.; Silin, V.; Meuse, C. W. *Langmuir* **2003**, 19, 3752.
- (7) Harder, P.; Grunze, M.; Dahint, R.; Whitesides, G. M.; Laibinis, P. E. *J. Phys. Chem.* **1998**, 102, 426.
- (8) Wang, R. L. C.; Kreuzer, H. J.; Grunze, M. *Phys. Chem. Chem. Phys.* **2000**, 2, 3613.

- (9) Vanderah, D. J.; Valincius, G.; Meuse, C. W. *Langmuir* **2002**, *18*, 4674.
- (10) Herrwerth, S.; Eck, W.; Reinhardt, S.; Grunze, M. *J. Am. Chem. Soc.* **2003**, *125*, 9359.
- (11) Valiokas, R.; Svedhem, S.; Svensson, S. C. T.; Liedberg, B. *Langmuir* **1999**, *15*, 3390.
- (12) Valiokas, R.; Östblom, M.; Svedhem, S.; Svensson, S. C. T.; Liedberg, B. *J. Phys. Chem. B* **2001**, *105*, 5459.
- (13) Lahiri, J.; Kalal, P.; Frutos, A. G.; Jonas, S. J.; Schaeffler, R. *Langmuir* **2000**, *16*, 7805.
- (14) Valiokas, R.; Vaitekoniš, Š.; Klenkar, G.; Trinkūnas, G.; Liedberg, B. *Langmuir* **2006**, *22*, 3456.
- (15) Benesch, J.; Svedhem, S.; Svensson, S. C. T.; Valiokas, R.; Liedberg, B.; Tengvall, P. *J. Biomater. Sci., Polym. Ed.* **2001**, *12*, 581.
- (16) Zheng, J.; Li, L.; Tsao, H.-K.; Sheng, Y.-J.; Chen, S.; Jiang, S. *Biophys. J.* **2005**, *89*, 158.
- (17) Valiokas, R.; Östblom, M.; Björefors, F.; Liedberg, B.; Shi, J.; Konradsson, P. *Biointerphases* **2006**, *1*, 22.
- (18) Zhang, F.; Skoda, M. W. A.; Jacobs, R. M. J.; Zorn, S.; Martin, R. A.; Martin, C. M.; Clark, G. F.; Goerigk, G.; Schreiber, F. *J. Phys. Chem. A* **2007**, *111*, 12229.
- (19) Malysheva, L.; Onipko, A.; Valiokas, R.; Liedberg, B. *J. Phys. Chem. A* **2005**, *109*, 7788.
- (20) Wang, R. L. C.; Kreuzer, H. J.; Grunze, M. *J. Phys. Chem.* **1997**, *101*, 9767.
- (21) Malysheva, L.; Onipko, A.; Valiokas, R.; Liedberg, B. *J. Phys. Chem. B* **2005**, *109*, 13221.